DNS AND LES OF THE TRANSITION PROCESS IN A LAMINAR SEPARATION BUBBLE

Olaf Marxen and Ulrich Rist
Institut für Aerodynamik und Gasdynamik, Universität Stuttgart, D-70550 Stuttgart, Germany
olaf.marxen@iag.uni-stuttgart.de, rist@iag.uni-stuttgart.de

Abstract A region of strong local adverse pressure gradient acting on a laminar flat-plate boundary layer can produce a closed fully laminar separation bubble for sufficiently small pressure rise and Reynolds number. However, such a flow field is hydrodynamically highly unstable and transition will occur in the region of adverse pressure gradient. Due to an interaction with the potential flow, the transition process may even suppress laminar separation completely.

Direct numerical simulation (DNS) of oblique transition in a steady laminar separation bubble is carried out. The mean flow deformation is found to play an important role even upstream of the transition location. However, with proper treatment of the upper boundary it is possible to take the upstream influence into account and to obtain results that are height independent in accordance with the physical model of an unbounded domain. Hence, DNS results can serve as a reference for an analysis of the large-eddy simulation (LES) technique.

Such an analysis of LES is carried out based on a (scale) separation step associated with an explicit filter and a (subfilter-scale) modeling step to obtain closure. It is shown that filtering of the Navier-Stokes equations is not a formality and that the subgrid-scale model has to be adopted to the filter accordingly. Numerical results for a discrete filter together with a relaxation term model lead to guidelines for the choice of the explicit filter and the desired action of the turbulence model.

Keywords: transition, laminar separation bubble, DNS, LES

Introduction

A laminar boundary layer separates in a region of adverse pressure gradient on a flat plate and can reattach while being still laminar in case of a sufficiently small pressure rise and low Reynolds number, forming a laminar separation bubble (LSB). However, such a flow field is hydrodynamically unstable and will amplify incoming disturbances by several orders of magnitude. Therefore, the laminar separation bubble is likely to be the location of transition to turbulence. Through its upstream influence, in some cases the transition process is able to completely suppress separation by an interaction of the mean flow deformation with the potential flow (so-called vicous-inviscid interaction).

Numerical techniques applied to as complex as separated and transitional flows rely mainly on direct numerical simulations (DNS, see e.g. Alam and Sandham, 2000) to keep uncertainties connected with a turbulence model to a minimum. In many technical applications laminar separation plays an important role, e.g. on low pressure turbine blades. Thus, there is need for numerical methods to accurately capture the behaviour of laminar separation bubbles that are less expensive than DNS. One of these methods is the so-called large-eddy simulation that aims at capturing the motion of large coherent structures while modeling the small-scale turbulence. Only a few large-eddy simulations (LES) of LSB's are reported in literature (Yang and Voke, 2001, Wilson and Pauley, 1998). A detailed comparison of results from both techniques for a flow field where DNS is still feasible to provide a reference can serve to shed light on modeling uncertainties. The first part of the paper addresses issues related to establishing a proper reference case by means of DNS.

The methodology of LES consists of two steps: separation of variables into resolved and unresolved scales (*separation step*) by application of a spatial filter, and replacing the resulting unclosed (subgrid- or subfilter-scale) stresses by a turbulence model (*modeling step*). For a long time, the separation step was considered a mere formality and its quantitative effect on the solution of the equations of motion has only recently drawn more attention (Pruett, 2001). The present work aims at analysing the quantitative effect of isolated parts of the LES method on the numerical results. This is beliveved to provide deeper insights compared to a full LES run with its complex interaction of filter, model, and discretization strategy. Dependence of the results on turbulence model and (explicit) filtering operation will be discussed in the second part of the paper.

1. Numerical Method and Definiton of the Base Flow

Numerical Method. Spatial direct numerical simulation of the full three-dimensional Navier-Stokes equations in vorticity-velocity formulation were carried out in a disturbance formulation for incompressible flow. All quantities are divided into a steady part $U_b(x, y)$ and a fluctuation $u(x, y, z)$. Finite differences (4^{th}/6^{th} order) on a Cartesian grid are used in streamwise and wall-normal direction while a spectral ansatz is applied in spanwise direction. An explicit fourth-order Runge-Kutta scheme is used for time integration. Upstream of the outflow boundary a buffer domain smoothly ramps down all disturbances. These disturbances are introduced via blowing/suction through a narrow slot in the wall near the inflow boundary. Details of the numerical method can be found in Kloker, 1998. In addition, grid stretching is applied in wall-normal direction (Meyer, 2003).

Definition of the Base Flow. A generic test case was chosen that has already been well-studied by means of DNS (Rist and Maucher, 1994). It models a physical situation as shown in Fig. 1. All quantities are non-dimensionalized resulting in a Reynolds number Re=10^5. The streamwise axis x is denoted as for a Blasius boundary layer. To illustrate this, c_f-values for the Blasius solution are added to Fig. 2. In contrast to Rist and Maucher, 1994, the integration domain starts slightly further downstream at x_0=1.021576 and ends at x_e =3.36468. The Reynolds number based on the displacement thickness δ_1 at the infbw boundary is $Re_{\ \delta_1}$=570. The domain height equals y_{max}=$\Delta_M \cdot \delta_1$ with Δ_M=23.2 at the infbw boundary. Characteristic boundary-layer parameter distributions are given in Fig. 2. Boundary-layer thicknesses (e.g. δ_1) are computed based on the spanwise vorticity (see Spalart and Strelets, 2000).

The fbw fi eld was obtained from a calculation where a distribution for the streamwise velocity was prescribed at the upper boundary to impose the pressure gradient. The calculation was advanced until a steady state was reached. Using this steady laminar solution as a base fbw, the unsteady development with controlled disturbance input is computed as discussed in the next section.

2. Direct Numerical Simulation of Transition in a LSB

Disturbance Input and Resolution Requirement. The transition scenario studied here is similar to the oblique case O in Rist and Maucher, 1994. Below, the notation (h, k) will be used to denote modes with h-times the fundamental frequency $\beta = 18$ and k-times the fundamental spanwise wave number $\gamma = 40$. A single pair of oblique waves $(1, \pm 1)$ is introduced in a disturbance strip between $x = 1.152475$ and $x = 1.283375$ with a v-amplitude of $A_v = 2 \cdot 10^{-4}$ each. The buffer domain started at $x = 3.102881$.

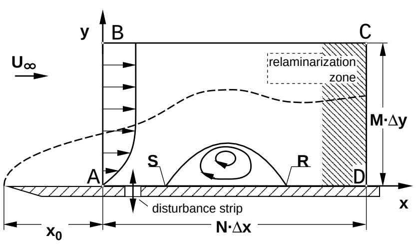

Figure 1. Physical configuration.

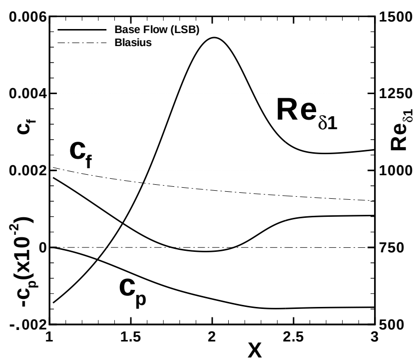

Figure 2. Base flow values for surface pressure c_p, skin friction coefficient c_f, and local Reynolds number Re_{δ_1}.

The DNS was carried out with N=1970 grid points in streamwise direction, M=225 grid points in wall-normal direction and K=63 (complex, i.e. asymmetric) spanwise modes. In wall-normal direction grid points were clustered at the wall. Resolution in time was 1600 time steps per fundamental period.

Results were highly sensitive to underresolution in wall-normal direction (not shown). However, 15 (real, i.e. symmetric) spanwise modes proved to be suffi cient to predict correct mean values shortly beyond the transition location (Fig. 3), while showing an overshoot in the skin friction in the turbulent part. The calculation was advanced for at least 20 periods before analysing the data to get rid of initial transients, visible e.g. as mode $(0.5, 0)$ in Fig. 4.

Mean Flow Deformation and Upper Boundary. The small disturbance input is suffi cient to completely suppress separation (Fig. 3). In particular, it is remarkable that the mean fbw deformation (MFD) (mode $(0, 0)$ in the present notation) is the largest observable disturbance even far upstream around the location of the disturbance strip (Fig. 4). Such an effect was not observed for subharmonic or fundamental breakdown that lead to saturated spanwise rollers but not to true turbulent fbw (Rist, 1998), were a relatively small deviation of mean fbw values was seen only downstream of disturbance saturation.

Because of the importance of the MFD even at the upper boundary, the original formulation of the upper boundary condition $\frac{\partial v}{\partial y} = -\alpha v$ was replaced by a boundary-layer interaction model. It is based on a source/sink distribution at the wall, which strongly depends on the disturbances introduced. With such a boundary condition independence on the domain height could be obtained (Fig. 3). This independence is important since the underlying physical model is a boundary layer with an adverse pressure gradient, i.e. an unbounded domain, and not a channel fbw.

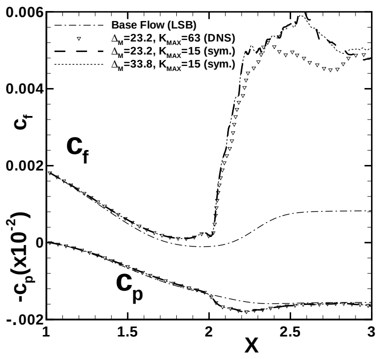

Figure 3. Comparison of c_p and c_f for two different spanwise resolutions K=15 and K=63 and two different domain heights Δ_M=23.2 and Δ_M=33.8.

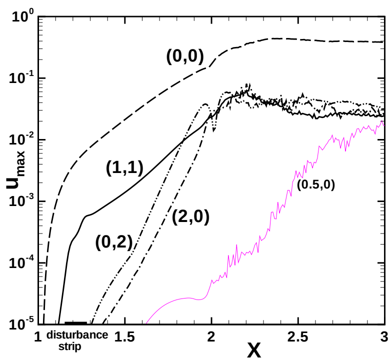

Figure 4. Amplification of the max. streamwise velocity fluctuation u_{max} for the DNS (K=63, Δ_M=23.2).

3. Analysis of Large-Eddy Simulation

The DNS solution presented in the last section will serve as a reference for the following analysis of LES. This analysis is carried out according to the two steps introduced before. In the next paragraphs, a filter operation is defined as the convolution integral:

$$u_i^*(x) = G_2 * u_i = \int G_2(\frac{x - x'}{\Delta}, x)\, u_i(x')\frac{dx'}{\Delta}. \quad (1)$$

Derivation of the Filtered Equations. Even though the calculations discussed in this paper were obtained with the vorticity-velocity formulation of the Navier-Stokes equations, derivation of the equations for LES will be demonstrated for primitive variables since this is more familiar in the literature. For numerical simulations the curl of the equations is taken and only commutative filters are applied. Starting point are the momentum equations:

$$\frac{\partial u_i}{\partial t} + \frac{\partial u_j u_i}{\partial x_j} + \frac{\partial p}{\partial x_i} - \frac{1}{Re}\frac{\partial^2 u_i}{\partial x_k x_k} = 0. \quad (2)$$

First, the *(scale) separation step* is carried out by adding a term to both sides of the equations (bold in eq. (3)), which is similar to the non-linear term, however with the velocities replaced by their filtered counterpart $u_i^* = G_2 * u_i$ (Fig. 5). The resulting equation is filtered with a spectral filter with cut-off wave number k_c. Spectrally filtered variables will be denoted by a tilde: $\tilde{u}_i = G_S * u_i$ (analogous to eq. (1)). With the additional constraint that the transfer function of G_2 is (only) 0 for $k > k_c$, the following equality holds: $u_i^* = G_2 * u_i = G_2 * \tilde{u}_i = \tilde{u}_i^*$. Note that the resulting equations are still exact, assuming we prescribe periodic boundary conditions:

$$\underbrace{\frac{\partial \tilde{u}_i}{\partial t} + \frac{\partial \widetilde{\mathbf{\tilde{u}_j^* \tilde{u}_i^*}}}{\partial \mathbf{x_j}} + \frac{\partial \tilde{p}}{\partial x_i} - \frac{1}{Re}\frac{\partial^2 \tilde{u}_i}{\partial x_k x_k}}_{\text{dependent on scales } k < k_c \text{ only}} = \underbrace{\frac{\partial \widetilde{\mathbf{\tilde{u}_j^* \tilde{u}_i^*}}}{\partial \mathbf{x_j}} - \frac{\partial \widetilde{u_j u_i}}{\partial x_j}}_{\text{dependent on all scales } k}. \quad (3)$$

If eq. (3) would be solved on a grid that can resolve scales up to $k = k_c$, the right-hand side of that equation would be the so-called subgrid-scale term (SGS term). The second term on the left-hand side cannot generate scales $k \geq k_c$ and does not depend on them. Furthermore, formally eq. (3) does not depend on the choice of G_2 while the quantitative value of the right-hand side will. Thus, it could as well be called the subfilter-scale term.

The second step is the *(subfilter-scale) modeling step*. The right hand side will be replaced by a term that depends only on scales below the cut-off k_c to obtain closure. In the LES terminology, such a term is called a turbulence or SGS model. One simple model is a so-called relaxation term, e.g. $\chi\,(\tilde{u}_i^* - \tilde{u}_i)$:

$$\frac{\partial \tilde{u}_i}{\partial t} + \frac{\partial \widetilde{\tilde{u}_j^* \tilde{u}_i^*}}{\partial x_j} + \frac{\partial \tilde{p}}{\partial x_i} - \frac{1}{Re}\frac{\partial^2 \tilde{u}_i}{\partial x_k x_k} = \chi\,(\tilde{u}_i^* - \tilde{u}_i)\,. \tag{4}$$

Note that all necessary steps have been carried out now, solving eq. (4) will be called a LES. For constant χ only(!) the right-hand side acts purely dissipative. In that case, the present closure can be related to the approximate deconvolution model (ADM) (Stolz et al., 2001a; Stolz et al., 2001b). However, to arrive at the equations used in ADM, another filter G has to be applied to eq. (4): $\bar{u}_i = G * u_i$. With the constraint that $G_2 = Q_N * G$ and $Q_N = \sum_{\nu=0}^{N}(1-G)^\nu$, one obtains:

$$\frac{\partial \bar{u}_i}{\partial t} + \overline{\frac{\partial u_j^* u_i^*}{\partial x_j}} + \frac{\partial \bar{p}}{\partial x_i} - \frac{1}{Re}\frac{\partial^2 \bar{u}_i}{\partial x_k x_k} = -\chi\,(I - Q_N * G) * \bar{u}_i, \tag{5}$$

$$\text{with } \bar{\tilde{u}}_i = \bar{u}_i = I * \bar{u}_i,$$
$$\bar{\tilde{u}}_i^* = G * (Q_N * G * \tilde{u}_i) = (G * Q_N) * \bar{u}_i = (Q_N * G) * \bar{u}_i.$$

Numerical Results. From what has been shown in the last paragraph it is obvious that the last step (to arrive at the ADM equations) is not necessary, and with it the whole procedure of filtering and deconvolution, since closure was obtained already in the second step. This was earlier recognized by Winckelmans and Jeanmart, 2001. In particular, eq. (4) and eq. (5) will yield equal results, if the solution of eq. (4) is filtered in a postprocessing step.

This was checked by applying the filtering only in the spanwise direction using 15 Fourier harmonics (K=15=$k_c - 1$), where the present numerical method

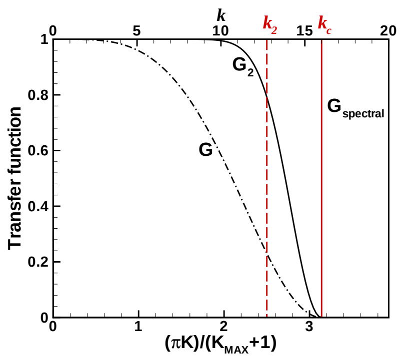

Figure 5. Filter transfer functions as a function of wave number.

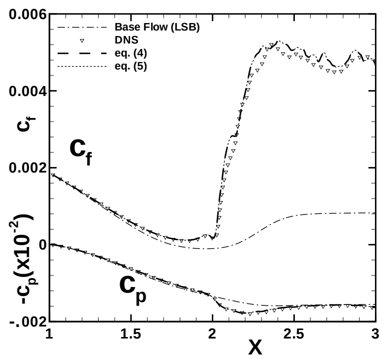

Figure 6. Results of eq. (4) and eq. (5) for K=15, filtering in z only.

is in accordance with the assumption of periodicity. The turbulence model is given by the relaxation term with constant $\chi = 572.96 = \frac{\Delta t}{4}$. As a filter G, a symmetric 5 point stencil was used, applied in Fourier space via its transfer function (Fig. 5), so that the integral in eq. (1) reduces to a product for each Fourier harmonic. Results show that solution of eq. (4), G_2 obtained from $Q_N * G$ with N=5, and eq. (5) are in fact equal as expected (Figs. 6, 7).

The spectrum (Fig. 7) reveals that the present LES is under-dissipative in the medium wave-number range $(5 \ldots 10)$. Such a behaviour was also observed by Winckelmans and Jeanmart, 2001. In the following an explanation is suggested. If k_2 is the cut-off wave number of G_2, the relaxation term in eq. (4) affects only scales $k{>}k_2$. However, filtering of the velocities $\tilde{u} \to \tilde{u}^*$ before plugging them into the non-linear term on the left-hand side will affect scales $k{<}k_2$ by suppressing an influence of scales in the range $k{>}k_2$ on them. Assuming that this effect would have been dissipative (i.e. scales in the range $k{>}k_2$ would act in a way as to draw energy from scales $k{<}k_2$), the complete model is not dissipative enough for scales $k{<}k_2$. Setting χ=0 or leave the non-linear term on the left-hand side unfiltered does not change the situtation significantly (Fig. 8), since both relaxation and explicit filtering act in a similar manner.

4. Conclusions

DNS of laminar-turbulent transition in a separation bubble was carried out. A large mean flow deformation reaching far upstream was observed and attributed to a viscous-inviscid interaction. This lead to a formulation of the upper boundary to yield height-independent results. The DNS-result was chosen as a reference case for a subsequent analysis of LES. This analysis consisted of two steps: a (scale) separation and a (subfilter-scale or SGS) modeling step. The first step is associated with an explicit filter applied to the non-linear

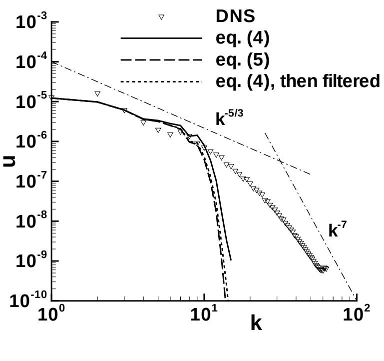

Figure 7. Spanwise spectra for the streamwise velocity integrated over the interval $[x = 2.5, 2.75; y = 0, y_{max}]$.

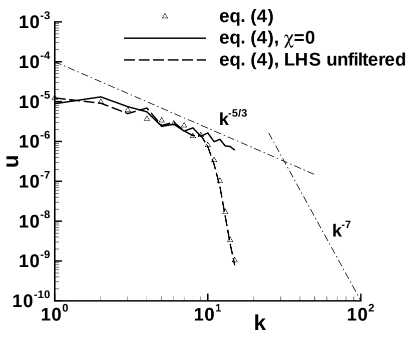

Figure 8. Same as Fig. 7. Results of eq. (4) for K=15, $\chi = 0$ and LHS unfitered.

term while the second step yields closure through a turbulence model. It was shown that the form of the filtered momentum equations does not depend on the choice of the filter while the quantitative value of the SGS model will.

From the observations made, the following guidelines for the choice of the filter G_2 and the SGS-model can be derived: G_2 should be designed such that $k_2 \leq min(\frac{2}{3}k_c, k^{FD}_{accurate})$ and the turbulence model should not only act on scales $k > k_2$ but also on smaller ones. The constraint on G_2 reduces errors originating from aliasing and finite differencing (k^{FD} is the modified wave number), while the modeling aspect was discussed in the previous section.

Acknowledgments

Financial support of this research by the Deutsche Forschungsgemeinschaft DFG under grant Ri 680/10-2 is gratefully acknowledged.

References

Alam, M. and Sandham, N. (2000). Direct Numerical Simulation of 'Short' Laminar Separation Bubbles with Turbulent Reattachment. *J. Fluid Mech.*, 410:1–28.

Kloker, M. (1998). A robust high-resolution split-type compact FD scheme for spatial direct numerical simulation of boundary-layer transition. *Appl. Sci. Res.*, 59:353–377.

Meyer, D. (2003). *Direkte numerische Simulation nichtlinearer Transitionsmechnismen in der Strömungsgrenzschicht einer ebenen Platte*. Dissertation, Universität Stuttgart.

Pruett, C. (2001). Toward the de-mystification of LES. In Liu, C., Sakell, L., and Beutner, T., editors, *DNS/LES Progress and Challenges*, page 231. Greyden, Columbus, OH.

Rist, U. (1998). Zur Instabilität und Transition in laminaren Ablöseblasen. Habilitation, Universität Stuttgart, Shaker Verlag, Aachen.

Rist, U. and Maucher, U. (1994). Direct numerical simulation of 2D and 3D instability waves in a laminar separation bubble. In *Application of Direct and Large Eddy Simulation to Transition and Turbulence*, number AGARD CP-551, pages 34.1–7. 74th Fluid Dynamics Symposium.

Spalart, P. and Strelets, M. (2000). Mechanisms of Transition and Heat Transfer in a Separation Bubble. *J. Fluid Mech.*, 403:329–349.

Stolz, S., Adams, N., and Kleiser, L. (2001a). An approximate deconvolution model for large-eddy simulation with application to incompressible wall-bounded flows. *Phys. Fluids*, 13(4): 997–1015.

Stolz, S., Adams, N., and Kleiser, L. (2001b). The approximate deconvolution model for large-eddy simulation of compressible flow and its application to shock-boundary-layer interaction. *Phys. Fluids*, 13(10):2985–3001.

Wilson, P. and Pauley, L. (1998). Two- and three-dimensional large-eddy simulations of a transitional separation bubble. *Phys. Fluids*, 10(11):2932–2940.

Winckelmans, G. and Jeanmart, H. (2001). Assessment of some models for LES without/with explicit filtering. In Geurts, B., Friedrich, R., and Metais, O., editors, *Direct and Large-Eddy Simulation - IV*, volume 8, pages 55–66. Ercoftac Series, Kluwer Academic Publishers, Dordrecht, Boston, London.

Yang, Z. and Voke, P. (2001). Large-Eddy Simulation of Boundary-layer and Transition at a Change of Surface Curvature. *J. Fluid Mech.*, 439:305–333.